SYNTHESIS AND CHARACTERIZATION OF CHITOSAN/SODIUM ALGINATE BLEND MEMBRANE FOR APPLICATION IN AN ELECTROCHEMICAL CAPACITOR

Krzysztof Nowacki*, Maciej Galiński, Izabela Stępniak

Poznan University of Technology, Institute of Chemistry and Technical Electrochemistry
ul. Berdychowo 4, 60-965 Poznan, Poland

**e-mail: krzysztof.j.nowacki@doctorate.put.poznan.pl*

Abstract

In this work, we report a stepwise formation method of a chitosan/sodium alginate polyelectrolyte complex (CS/SA PEC) membrane. The proposed method aiming at the utilization of the ultrasonic treatment of chitosan and sodium alginate solution allowed us to obtain a highly homogeneous hybrid membrane for electrochemical usage. The CS/SA PEC membrane saturated in a 2 M Li_2SO_4 aqueous solution was used in electrochemical double layer capacitor (EDLC) cell to study its applicability as quasi-solid electrolyte. Electrochemical characteristic of EDLC cells was determined by electrochemical impedance spectroscopy, cyclic voltammetry and galvanostatic charge/discharge methods. The results show that the EDLC cell with CS/SA PEC quasi-solid electrolyte exhibit a comparable specific capacitance (102 F g^{-1} for 0–0.8 V) to CS reference (100 F g^{-1} for 0–0.8 V) and commercial separator (99 F g^{-1} for 0–0.8 V) cells. Thus, the CS/SA PEC membrane can be considered as an alternative modification for chitosan-based materials of electrochemical purpose.

***Keywords**: chitosan, sodium alginate, electric double layer capacitor, supercapacitor, gel electrolyte, lithium sulfate*

Received: 14.03.2020
Accepted: 17.06.2020

1. Introduction

In recent years, the polymers of natural origin (biopolymers) have been one of the most investigated materials in medical science [1, 2]. Among them, highly abundant marine biopolymers such as chitin and alginate have been widely studied for their nontoxicity, biodegradability and biocompatibility [3–5]. At the same time, derivatives of chitin and alginic acid (chitosan and sodium alginate, respectively) are easily soluble in aqueous solvents, a feature that has attracted even more attention in high-end technology, due to their ease of chemical modification [6, 7]. Thus, these two biopolymers are often applied as vital components of bio-inspired elements in electrochemical devices such as fuel cells, supercapacitors and biosensors [8–11].

Chitosan is one of the most abundant natural polysaccharides; it is obtained from partial alkaline N-deacetylation of chitin, and as a natural cationic polymer, it has both reactive amino and hydrophilic hydroxyl groups [12]. The polycationic structure of chitosan confers an excellent ability to form gels [13]. Due to this unique property and additionally boosted by possible chemical modifications, this biopolymer has been the subject of intense research as a base material for forming quasi-solid electrolytes for electrochemical devices (mainly supercapacitors) [14, 15]. Unfortunately, unmodified chitosan is fragile and has relatively low mechanical strength in a swollen state. To overcome these problems, chitosan-based materials for electrochemical applications are modified by various methods [16, 17].

Sodium alginate is a sodium salt of alginic acid, an anionic polysaccharide derived mainly from cell walls of seaweeds [18]. Alginic acid, a natural biopolymer comprised of β-D-mannuronic acid and α-L-guluronic acid monosaccharide units, is insoluble in water and in living organisms it occurs in the form of a gel neutralized with calcium (Ca^{2+}), magnesium (Mg^{2+}), strontium (Sr^{2+}) or barium (Ba^{2+}) ions [19]. However, the monovalent salts of alginic acid (i.e. sodium alginate) are easily soluble in water in certain pH conditions. This feature, along with the nontoxicity and biocompatibility of this biopolymer, have led to a wide investigation of it in terms of drug delivery systems and wound dressings [20, 21]. The polyanionic character of sodium alginate macromolecules allows it to form hydrogels; although similar to chitosan, the applicability of monovalent alginate salts is limited by certain drawbacks as high water solubility and low mechanical strength. These problems must be solved before sodium alginate could be used as a membrane material. They can be overcome by applying various modifications of this polysaccharide such as crosslinking or blending with another polymer to form a polyelectrolyte complex [22, 23].

Sodium alginate and chitosan are promising materials for bio-inspired components of electrochemical devices, especially due to their unequalled polyelectrolyte properties, which allows them to form gels, sponges and hetero-composites tailored for specific purposes: quasi-solid electrolytes and electrode binders for supercapacitors or multilayered membranes for fuel cells [24–26]. The chitosan/sodium alginate polyelectrolyte complex (CS/SA PEC) has been described as biodegradable and biocompatible and in addition reported stable in pH conditions that are corrosive for pure chitosan and sodium alginate [27, 28]. Therefore, we decided to utilize a CS/SA blended membrane as a quasi-solid electrolyte in electric double layer capacitor. However, keeping in mind numerous drawbacks of biopolymer applications in electrochemical devices, we also proposed a novel method of hybrid CS/SA PEC membrane synthesis. The membrane was formed by a complex method that was designed by combining mixing solution and evaporation of a solvent technique with well-known ultrasound irradiation treatment. The first stage involved mixing chitosan in acetic acid with aqueous sodium alginate solution to form

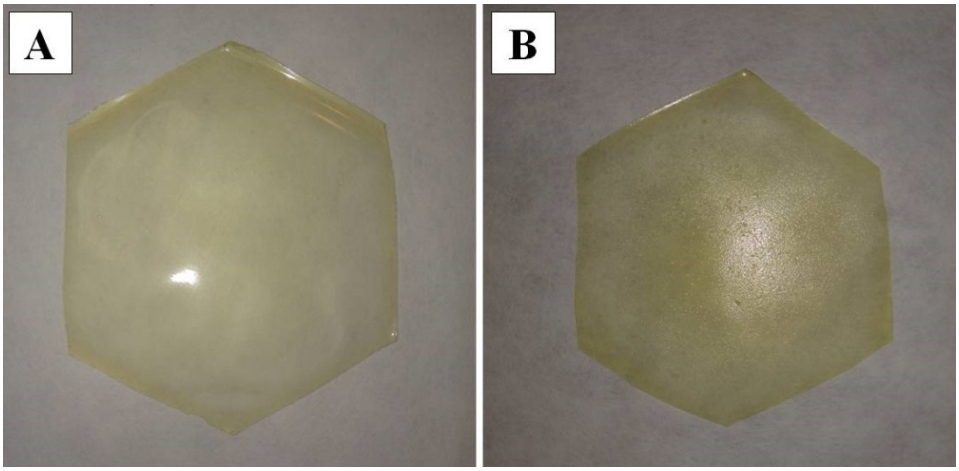

Figure 1. Samples of chitosan-based membranes: (A) chitosan and (B) chitosan/sodium alginate polyelectrolyte complex.

a polyelectrolyte complex. This reaction occurred due to electrostatic interactions of the carboxyl residues in the sodium alginate macromolecules with the amino groups of chitosan polymer chains [29]. Unfortunately, the uncontrolled formation of PEC during this stage caused by a rapid pH decrease (due to the acetic acid), insoluble conglomerates formed. The irregular distribution of these conglomerates could cause inhomogeneous performance of the membranes as quasi-solid electrolyte; therefore, the ultrasound treatment of the mixed solution was applied in a stage two. After ultrasonic homogenization and solvent evaporation, the synthesized membrane was utilized as electric double layer capacitor component.

2. Materials and methods

2.1. Chemicals

CS was purchased from Sigma-Aldrich and dried before use (105°C for 72 h). The physicochemical properties provided by the producer were degree of deacetylation 75%–85% and viscosity 200–800 cP in 1 wt% solution in 1% acetic acid (25°C). These parameters did not affect the further experiments and thus they were not more accurately analysed. SA powder was purchased from Sigma-Aldrich and dried before use (105°C for 72 h). Acetic acid (≥ 99.5%) and lithium sulfate (Li_2SO_4) (≥ 98.5) were also provided by Sigma-Aldrich and used for preparation of the aqueous solutions of CS and electrolyte, respectively. All reagents were used without further purification and redistilled water was used to prepare all aqueous solutions.

2.2. Preparation of CS Solution

A 2 wt% CS solution in 1 wt% aqueous acetic acid was prepared by dispersing an appropriate quantity of dry CS powder in acetic acid solution. The mixture was stirred for 336 h at 37°C until all CS powder was completely dissolved. A transparent, homogeneous solution with slightly yellow colour was obtained.

2.3. Preparation of a Raw CS Membrane

A raw CS membrane (Fig. 1A) was formed by solution casting and solvent evaporation techniques. In a standard procedure, 6 g of the homogeneous CS solution was poured into

a poly(propylene) mold, which was then left at 37°C for 24 h to evaporate the solvent. The dry CS membrane was carefully washed in 1:3 water:ethanol solution to remove acetic acid residue and dried under vacuum (25°C, 1 h).

2.4. Preparation of SA solution

A 0.2 wt% SA aqueous solution was prepared by dispersing an appropriate quantity of dry SA powder in redistilled water. The mixture was stirred for 6 h at 25°C until a transparent, homogeneous and colourless solution was obtained.

2.5. Preparation of CS/SA Membrane

A CS/SA PEC membrane (Fig. 1B) was obtained by a three-stage method. During the first stage, 6 g of homogeneous CS solution was mixed with 0.2 wt% SA aqueous solution in a predefined ratio of 1.25:1 by weight and was for 0.5 h. The second stage was realized by applying an ultrasound treatment using a Sonopuls HD 2070 homogenizer (Bandelin, Germany) for 10 min (20 kHz, 28 W). In stage three, the post-treated CS/SA solution after homogenization was poured into a poly(propylene) mold in order to evaporate the solvent. The subsequent steps were the same as in the formation of raw CS membrane (section 2.3).

2.6. Attenuated Total Reflectance-Fourier Transform Infrared Spectroscopy (ATR-FTIR)

Infrared spectroscopy analysis was used for the qualitative characterization of the CS and CS/SA PEC membranes. ATR-FTIR spectra were recorded on a Vertex 70 Series FTIR spectrometer (Bruker, Germany) from 4000–500 cm^{-1} with a resolution of 2 cm^{-1}.

2.7. X-Ray Diffraction (XRD)

The phase composition of the investigated membranes were characterized with an X-ray diffractometer using Cu $K_{\alpha 1}$ radiation at 30 kV and 25 mA anode excitation. The XRD patterns of samples were recorded at 25°C in the 2θ angle from 5 to 30°, with a step size of 0.04°/3 s.

2.8. Scanning Electron Microscopy (SEM)

Morphological properties of the samples were analysed with a SEM (HitachiS-3400N) equipped with an energy-dispersive detector and operated with an acceleration voltage from 10 to 15 kV. All samples were sputter-coated with graphite before SEM examination.

2.9 Electrolyte Uptake Test

The stability of the CS and CS/SA PEC membranes in an aqueous environment was evaluated using 2 M Li_2SO_4 solution. The vacuum-dried membranes were first characterized using an analytical scale (model AS 110.R2, Radwag, Poland) and Baker 130/7 thickness gauge, and then the samples were immersed in 1.5 mL of electrolyte solution for 94 h. The following measurements were performed in a specified time intervals (1/6, 1/3, 1/2, 1, 2, 4, 8, 24, 48 and 96 h). Before each measurement, excess solution from the membranes surface was removed by draining it off with a filter paper. The degree of swelling (DS) and thickness swelling ratio (DS_T) based on each measurement were calculated by using following equations:

$$DS\ (\%) = 100 \times (W_n - W_d) / W_d \text{ and} \quad (1)$$

$$DS_T\ (\%) = 100 \times (T_n - T_d) / T_d \quad (2)$$

where W_d and T_d represent the weight and thickness of the samples in a dry state, and W_n and T_n are the respective parameters of the examined membranes measured after a defined time of electrolyte treatment.

2.10. Ionic Conductivity Measurements

The ionic conductivity of the CS and CS/SA PEC membranes was evaluated by electrochemical impedance spectroscopy (EIS). The investigated samples (8 mm discs), previously swelled for 96 h in a 2 M Li_2SO_4 aqueous solution, were placed in a test vessel between two planar platinum electrodes (Fig. 2A). All measurements were performed at 25°C in the frequency range from 100 kHz to 1 Hz using blocking electrodes made of platinum (Pt) with a potential amplitude of 10 mV. Ionic conductivity (σ) of examined membranes was calculated as:

$$\sigma = s_s/(A \times R), \tag{3}$$

where s_s is the membrane thickness, A is the surface area of the working electrode (0.0177 cm^2) and R is the resistance of the membrane obtained from EIS measurements.

2.11. Assembly of Electric Double Layer Capacitor (EDLC) Test Cells

The electrochemical performance of the CS/SA PEC membranes as a quasi-solid electrolyte was analysed in an EDLC cell. For the experiment, a two-electrode Swagelok® system was adapted (Fig. 2B). Activated carbon cloth (Kynol® No ACC-507-20; 2000 m^2 g^{-1}) and Pt discs were utilized in test cells as an electrode material and current collectors, respectively. The CS/SA PEC membrane after 96 h treatment in a 2 M Li_2SO_4 aqueous solution was applied as a hydrogel electrolyte.

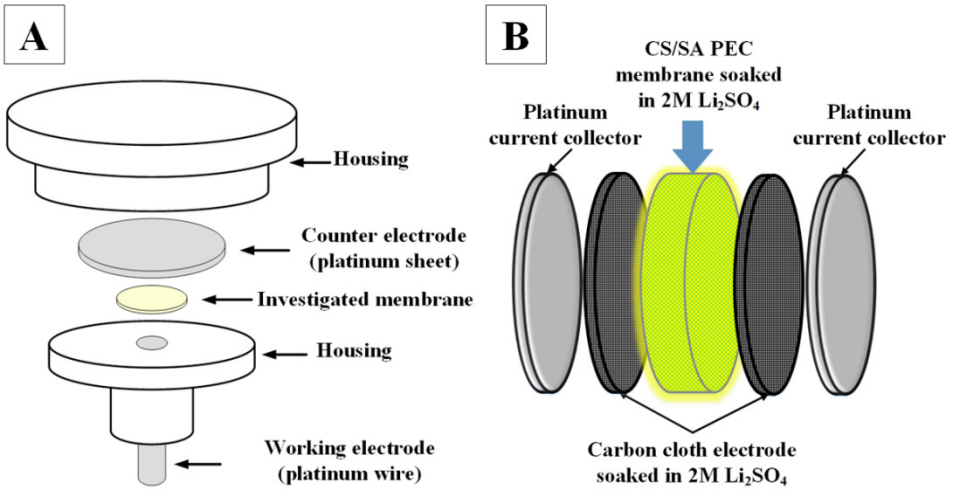

Figure 2. Schematic illustration of (A) the ionic conductivity measuring system and (B) an inside view of the electric double layer capacitor (EDLC) test cells assembled in this study.

For comparison, two more EDLC cells were assembled using the same electrode material and electrolyte as for CS/SA PEC cell. Specifically, one test cell with a raw CS membrane used a hydrogel electrolyte (pretreatment as for CS/SA PEC) and the second EDLC used a glass fibre membrane (Whatman GF/A), with a pore diameter of 1.6 μm and thickness of 0.3 mm, as a separator.

DOI: 10.15259/PCACD.25.014

2.12. Electrochemical Measurements

The electrochemical analysis of the CS and CS/SA PEC membranes in EDLC test cells were performed using EIS, cyclic voltammetry (CV) and galvanostatic charge/discharge (GCD) techniques. EIS was carried out using a μAutoLab FRA2 type III electrochemical system (EcoChemie, Netherlands) in the frequency range from 100 kHz to 0.01 Hz, with a potential amplitude of 10 mV. CV measurements were carried out using the same electrochemical system in the potential range from 0 to 0.8, 1.0, 1.2, 1.4 and 1.6 V, with different scan rates (5–100 mV s^{-1}). Chronoamperometric measurements were performed at a constant current of 5 mA with the cell voltage stepped from 0 to 0.8, 1.0, 1.2, 1.4 and 1.6 V, using an Atlas 0461 MBI multichannel electrochemical system (Atlas-Sollich, Poland). All electrochemical measurements were performed at room temperature (25 ºC).

3. Results and Discussion

3.1. ATR-FTIR

Spectra obtained using ATR-FTIR analysis for CS and CS/SA PEC membranes are demonstrated in Fig. 3. Both spectra feature characteristic bands for chitosan, such as amide I at 1636 cm^{-1}, identified as carbonyl stretching vibrations of N-acetyl groups. The presence of such bands as amide II (at 1546 cm^{-1}, νN-H), amide III (at 1328 cm^{-1}, νC-N) and a characteristic band for polysaccharides at 898 cm^{-1} (C–H deformation of the β-glycosidic bond, as well as the C–O–C bridge) additionally confirms a structure of a partially deacetylated chitosan [8]. Due to relatively low SA:CS mass ratio in the CS/SA PEC membrane, the characteristic for SA bands such as 1616 cm^{-1} (νC-O), 1417 cm^{-1} (νCOOH) and 1030 cm^{-1} (νC-O-C) are overlapped by the dominant chitosan spectrum [27]. However, the significant strengthening of a wide absorption band visible around 3247 cm^{-1} for the CS/SA PEC membrane (stretching vibrations of –OH and –NH)

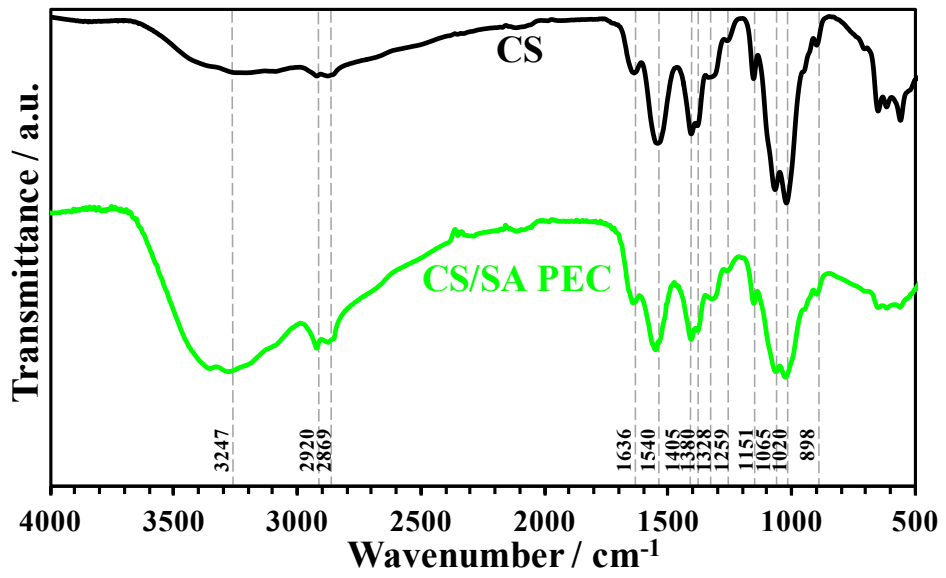

Figure 3. Attenuated total reflectance Fourier transform infrared spectroscopy spectra of chitosan (CS, black curve) and chitosan/sodium alginate polyelectrolyte complex (CS/SA PEC, green curve) membranes.

may be attributed to the reorganization of intermolecular hydrogen bonds between CS and SA due to formation of polyelectrolyte complex [30]. Thus, the slight differences in the wavelengths and intensity of the peaks in both spectra can also be related to this effect and provide additional confirmation of interactions between CS and SA molecules.

3.2. XRD Analysis

The XRD of raw CS powder and CS and CS/SA PEC membranes are shown in Fig. 4. Raw CS powder exhibited two typical broad diffraction peaks at 13.3 and 20.0°, which corresponds with literature data and confirms low crystallinity of the sample [27].

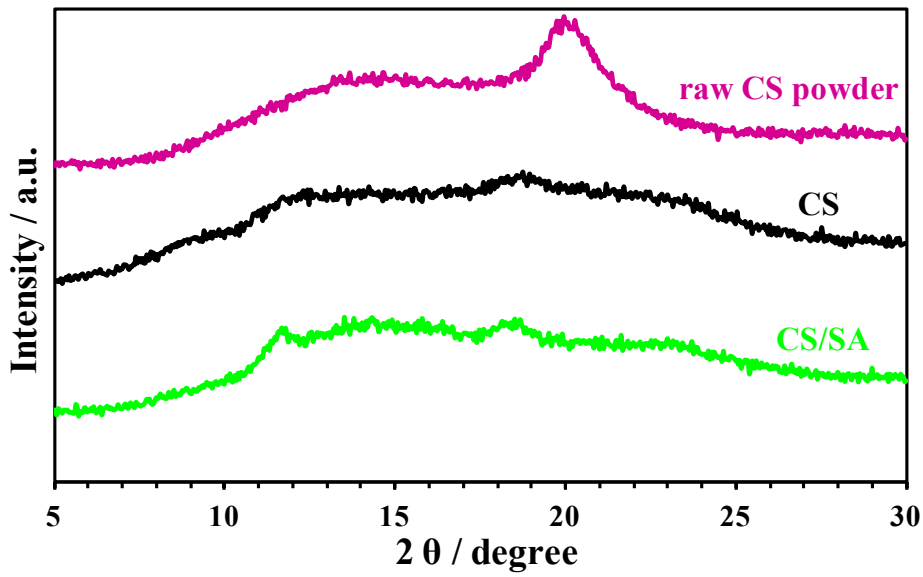

Figure 4. X-ray diffraction patterns of raw chitosan (CS) powder, CS and chitosan/sodium alginate polyelectrolyte complex (CS/SA PEC) membranes.

After the CS membrane formation, there was a marked intensity reduction of the 2θ ~20.0° peak; this change indicates that the processing reduces the crystalline nature of chitosan to an amorphous state [31]. The two main peaks overlap each other; therefore, there is no possibility to distinguish them and only one width band can be observed. Notwithstanding, there is a noticeable difference in the width of the bands between the CS/SA PEC and CS membrane diffraction patterns. This difference can provide information about the influence of the formation of PEC on the crystallinity within the sample. However, due to low SA mass addition and possible influence of other factors (drying, solvent), the visible reduction in the CS/SA PEC band width cannot be undeniably interpreted as the effect of formation of polyelectrolyte complex and ordering of the macromolecules within the polysaccharides blend.

3.3. SEM

The CS and CS/SA PEC dry membrane morphologies were investigated with SEM (Fig. 5). The general topography of both samples (Fig. 5A and B) showed a regular surface without defects or cracks. However, the CS/SA PEC membrane exhibited a rougher surface, with a regular distribution of unevenness, compared with the CS

membrane. This phenomenon can be caused by the uncontrolled formation of insoluble PEC conglomerates during membrane formation (mixing solution step). Nevertheless, the regular distribution of them might indicate that the ultrasonic treatment that allows for the sample to be easily homogenized. Further investigation of the membranes cross-sections (Fig. 5C and D) revealed a lamellar structure with conspicuous regular layers in all tested samples [32]. The view of the CS membrane cross-section presented more disordered spatial orientation of the layers and relatively larger gaps between them than the CS/SA PEC cross-section. This difference might indicate that the addition of SA to the CS matrix influences the membrane spatial network. Moreover, the cross-sectional SEM images illustrate that the ultrasonic treatment have no major influence on the membrane spatial morphology.

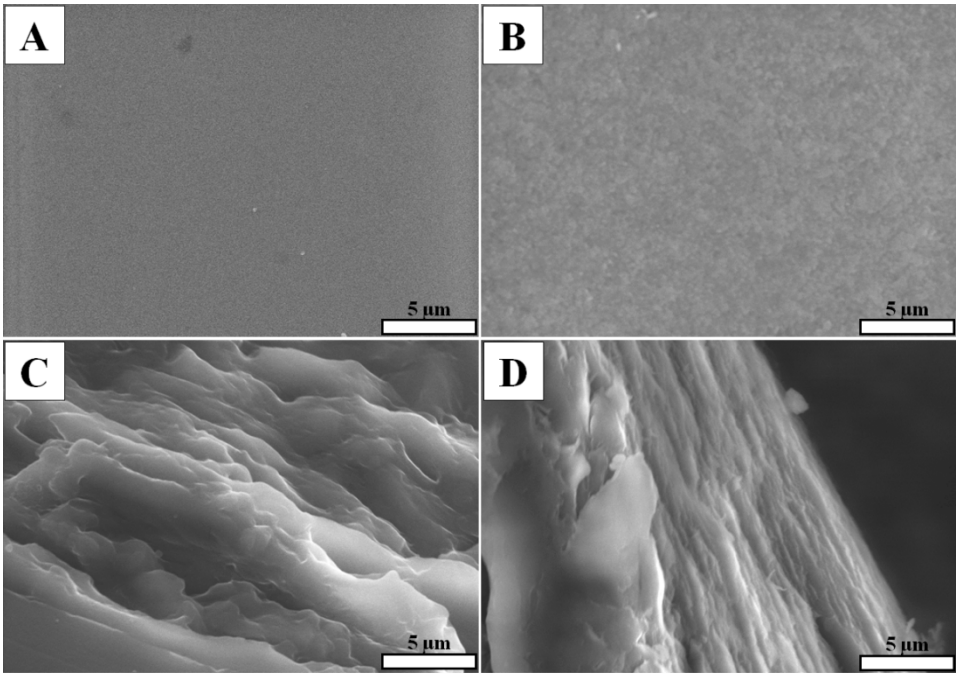

Figure 5 Scanning electron micrographs: (A) chitosan (CS) membrane surface, (B) chitosan/sodium alginate polyelectrolyte complex (CS/SA PEC) membrane surface, (C) CS membrane cross-section and (D) CS/SA PEC membrane cross-section.

3.4. Swelling Ratio

The data obtained from the electrolyte uptake test (in 2 M Li_2SO_4) indicated significant differences between the CS and CS/SA PEC membrane in terms of volumetric growth in an aqueous environment. The DS vs. time dependency graph (Fig. 6) revealed that the non-modified CS sample exhibited an extremely high DS (up to ~250% by mass). The CS membrane swelled rapidly; however, equilibrium for this sample was reached after 48 h of electrolyte treatment. This result implies that non-modified chitosan is not useful as a quasi-solid electrolyte material, due to excessive swelling and long equilibrium time. The DS values obtained for the CS/SA PEC membrane were significantly lower than those for raw chitosan (up to ~130% by mass).

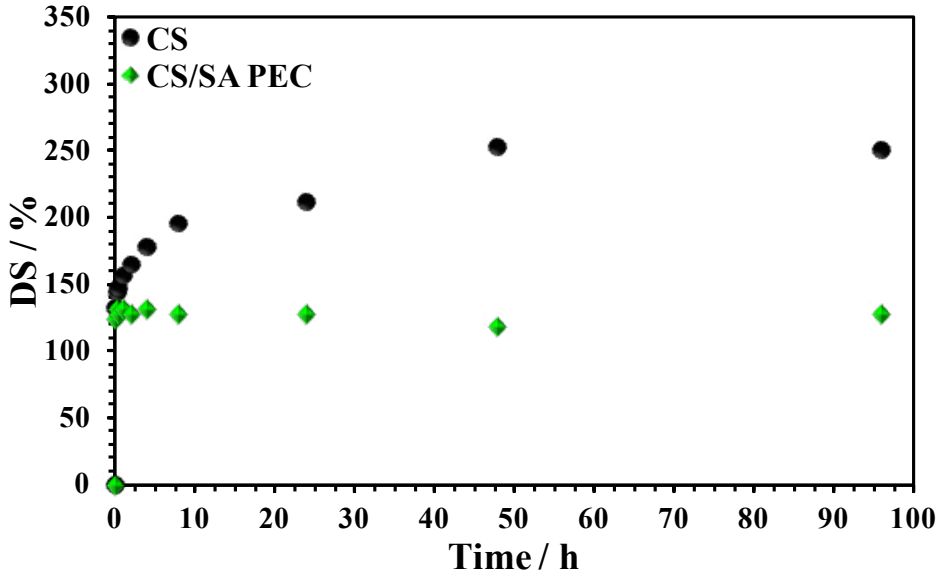

Figure 6. Degree of swelling (DS) vs. time of all tested membranes. Abbreviations: CS, chitosan; CS/SA PEC, chitosan/sodium alginate polyelectrolyte complex.

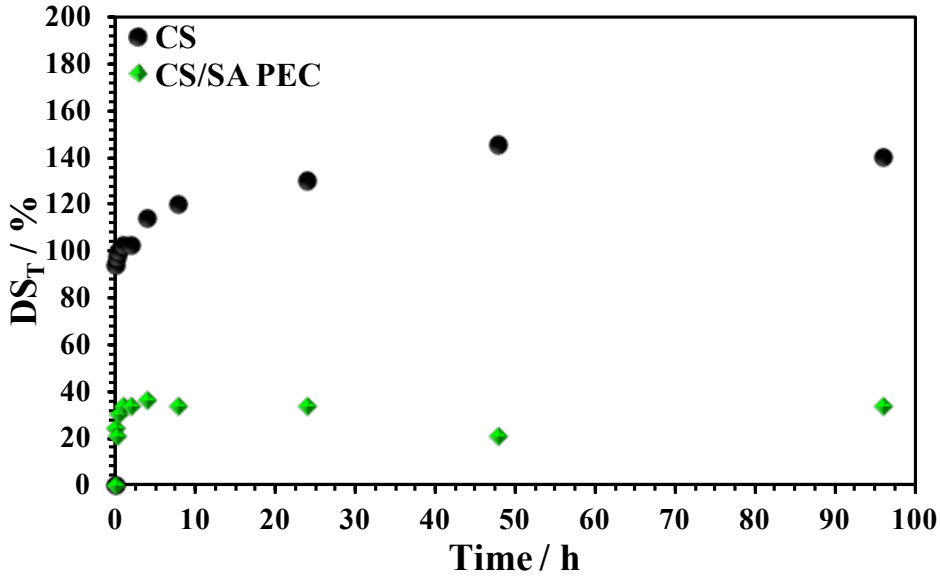

Figure 7. Thickness swelling ratio (DS_T) vs. time of all examined membranes. Abbreviations: CS, chitosan; CS/SA PEC, chitosan/sodium alginate polyelectrolyte complex.

Moreover, by comparing the plots of DS, the CS/SA PEC membrane reaches equilibrium state faster than the CS membrane (after 1 h of electrolyte treatment). This finding means that less electrolyte is absorbed by the CS/SA PEC membrane and that

infiltration of the 2 M Li_2SO_4 solution within this membrane is also rapid in the early stages. However, unlike the CS membrane, the chemical potential between the CS/SA PEC membrane and the electrolyte solution was quickly compensated. This effect is attributable to the incorporation of stabilizing SA polymer chains into the CS matrix, a phenomenon that greatly reduces the electrolyte uptake by stabilizing the spatial structure of the membrane with strong complexation interactions.

The thickness swelling ratio (DS_T) values showed similar trends to DS, and the equilibrium values for the CS (thickness in the dry state: 0.070 mm) and CS/SA PEC (thickness in the dry state: 0.066 mm) membrane were 146% and 33%, respectively. The difference in dynamic DS_T curves illustrates that it is essential to stabilize the three-dimensional structure of the CS polymer chains, in order to diminish the electrolyte absorption and exclude the impact of this process to membrane thickness. The CS/SA complexation seems to create strong, stabilizing interactions between this two biopolymers, and thus the CS/SA PEC membrane structure is more stable in the swelled state, which is important in view of its potential electrochemical applications [33].

3.5. Ionic Conductivity

From Fig. 6, there is a clear difference in electrolyte uptake between the CS and CS/SA PEC membrane. The impact of this phenomenon on the ionic conductivity of tested samples was evaluated by EIS (Table 1). The ionic conductivity of the CS/SA PEC hydrogel reached 18.70 mS cm^{-1}, which is nearly two times lower compared with the CS hydrogel (39.13 mS cm^{-1}). Based on the weight values of the swelled membranes, this effect is attributable to the amount of absorbed electrolyte [34]. One possible explanation is that the aqueous environment of unmodified CS membrane polymer chain network would weaken the electron transfer resistance by simply swelling and, consequently, create tunnels accessible for electrolyte ions. Therefore, the complexed CS/SA membrane, with a tight spatial network of polymeric chains, showed a significantly lower ionic conductivity than the reference sample. Moreover, ionic conductivity values of both CS-based membranes were significantly lower compared with the value of this parameter for dampened in the electrolyte Whatman GF/A separator (83.05 mS cm^{-1}).

Table 1. Ionic conductivity (σ) thickness in the swollen state (s_s) and mass (m_s) for examined membranes in 2 M Li_2SO_4 aqueous solution (96 h) and equivalent circuit (EC) used in EIS fitting method.

Membrane	σ [mS cm^{-1}]	s_s [cm]	m_s [g]	EC
CS	39.13	0.0150	0.0183	$R_1(R_2Q_1)$
CS/SA PEC	18.70	0.0084	0.0072	$R_1(R_2Q_1)$
Whatman GF/A	83.05	0.0300	0.0450	$R_1(R_2Q_1)$

Abbreviations: CS, chitosan; CS/SA PEC, chitosan/sodium alginate polyelectrolyte complex; GF/A, glass fibre.

3.6. Electrochemical studies

3.6.1. EIS

Fig. 8 displays the Nyquist plots for CS, CS/SA PEC and Whatman GF/A test devices. All obtained EIS spectra showed the typical shape for an EDLC [35]. In the high-frequency range, a semicircle is spotted, and in the low-frequency range, the EIS spectrum

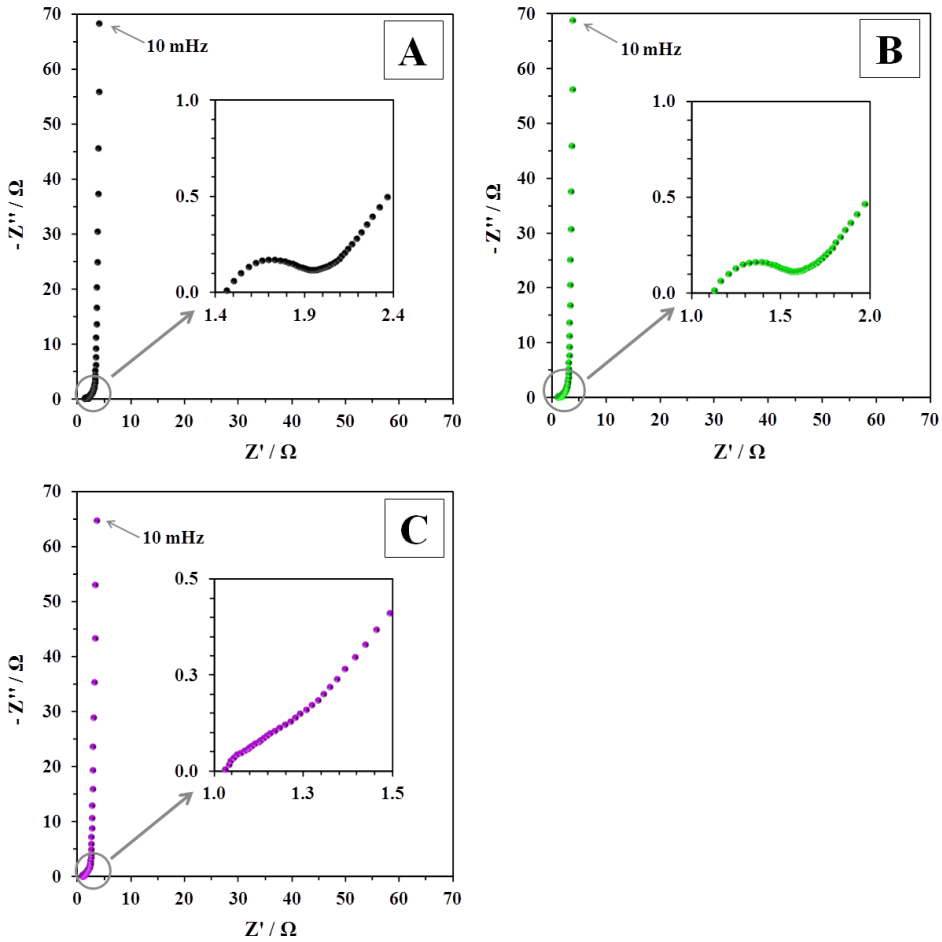

Figure 8. AC impedance spectra for capacitors with (A) CS, (B) CS/SA PEC membrane and (C) Whatman GF/A glass fiber separator. Abbreviations: Abbreviations: CS, chitosan; CS/SA PEC, chitosan/sodium alginate polyelectrolyte complex, GF/A, glass fibre.

is a straight line parallel to the imaginary axis. Therefore, a good capacitive behaviour can be expected for all tested EDLCs. The insets of Fig. 8A and B show a magnified high-frequency region of the EIS spectra; the origin of the semicircular curve can be explained by three independent factors: (i) the interfacial resistances of carbon material and (ii) connection of current collector and electroactive material as well as (iii) distribution of the pores structure and electrolyte resistance therein.

Therefore, the series resistance (R_s) is an important parameter for characterization of EDLC system performance; it can be easily determined by extrapolation of the high-frequency part of the EIS curve to the condition $Z' = 0$ [36]. Both reference capacitors, CS and Whatman GF/A, showed relatively low R_s: 1.46 Ω and 1.03 Ω, respectively. This phenomenon can be attributed to the high ionic conductivity of the swelled, non-modified CS membrane as well as the commercial glass fibre separator. Among the CS-based membranes, the lowest value of R_s was registered for capacitor test cell assembled with the CS/SA PEC quasi-solid electrolyte (1.13 Ω), although the CS/SA

PEC membrane exhibited lower values of ionic conductivity than the CS membrane. Given that R_s is associated with the ionic resistance across the partition between the two facing electrodes, this extraordinary result of the CS/SA PEC EDLC cell may be attributed to the thickness of the membrane in the swelled state. Analysis of the DS_T values (Fig. 7) revealed that the CS membrane in the equilibrium state swells over 4 times more than the CS/SA PEC in the direction of thickness. Thus, the limited swelling properties of the CS/SA sample could positively influence the bulk resistance of the quasi-solid electrolyte.

3.6.2. CV

Cyclic voltammograms at different scan rates (from 5 to 100 mV s^{-1}) registered for the CS/SA PEC test cell as well as CS and Whatman GF/A comparison cells are shown in Fig. 9A–C. Regarding the shape of this CV curves, the nearly ideal rectangular line for all EDLC characteristics (up to 10 mV s^{-1}) proves a good charge propagation in the potential range from 0 to 0.8 V. Moreover, the Whatman GF/A reference EDLC cell showed comparable CV characteristics with the CS/SA PEC membrane capacitor and there were no significant deviations (such as redox peaks). Thus, the assembled test capacitor cells should be treated in further calculations as regular EDLC devices [37].

Analysis of the cyclic voltammograms in Fig. 9A–C allowed us to predict the optimal scan rate for further CV curves with expanded potential range (up to 1.6V). Given that the deviation from the ideal box shape was the smallest for 10 mV s^{-1}, this value was utilized as a standard scan rate. Fig. 9D–F displays the cyclic voltammograms recorded in expanded potential range from 0 to 0.8, 1.0, 1.2, 1.4 and 1.6 V, for CS, CS/SA PEC and Whatman GF/A EDLCs. The CV curves exhibited the standard EDLC rectangular shape with visible deviations for higher potential values (over 1.0 V), which are probably caused by electrochemical decomposition of water. However, these peaks are relatively small compared with the whole voltammogram area. Thus, the tested EDLCs can be treated as a model system [38], and the specific capacitance values for all capacitor cells were calculated using the equation:

$$C_{sp} = \int I\mathrm{d}t/(\mathrm{d}E/\mathrm{d}t)m^{-1}, \quad (4)$$

where I is the current, $\mathrm{d}E/\mathrm{d}t$ is the potential scan rate and m is the mass of the active electrode material. Table 2 gathers obtained results and shows their dependency on the potential range.

Table 2 Specific capacitance (C_{sp}) of electrochemical double layer capacitor (EDLC) cells, calculated from a cyclic voltammetry.

EDLC	C_{sp} [F g^{-1}]				
	0–0.8 V	0–1.0 V	0–1.2 V	0–1.4 V	0–1.6 V
CS	97	122	145	171	203
CS/SA PEC	101	125	150	179	211
Whatman GF/A	98	122	150	176	209

Abbreviations: CS, chitosan; CS/SA PEC, chitosan/sodium alginate polyelectrolyte complex, GF/A, glass fibre.

There were small differences between specific capacitance values of CS and CS/SA PEC EDLCs. Nevertheless, the capacitor cell with the CS/SA PEC membrane showed

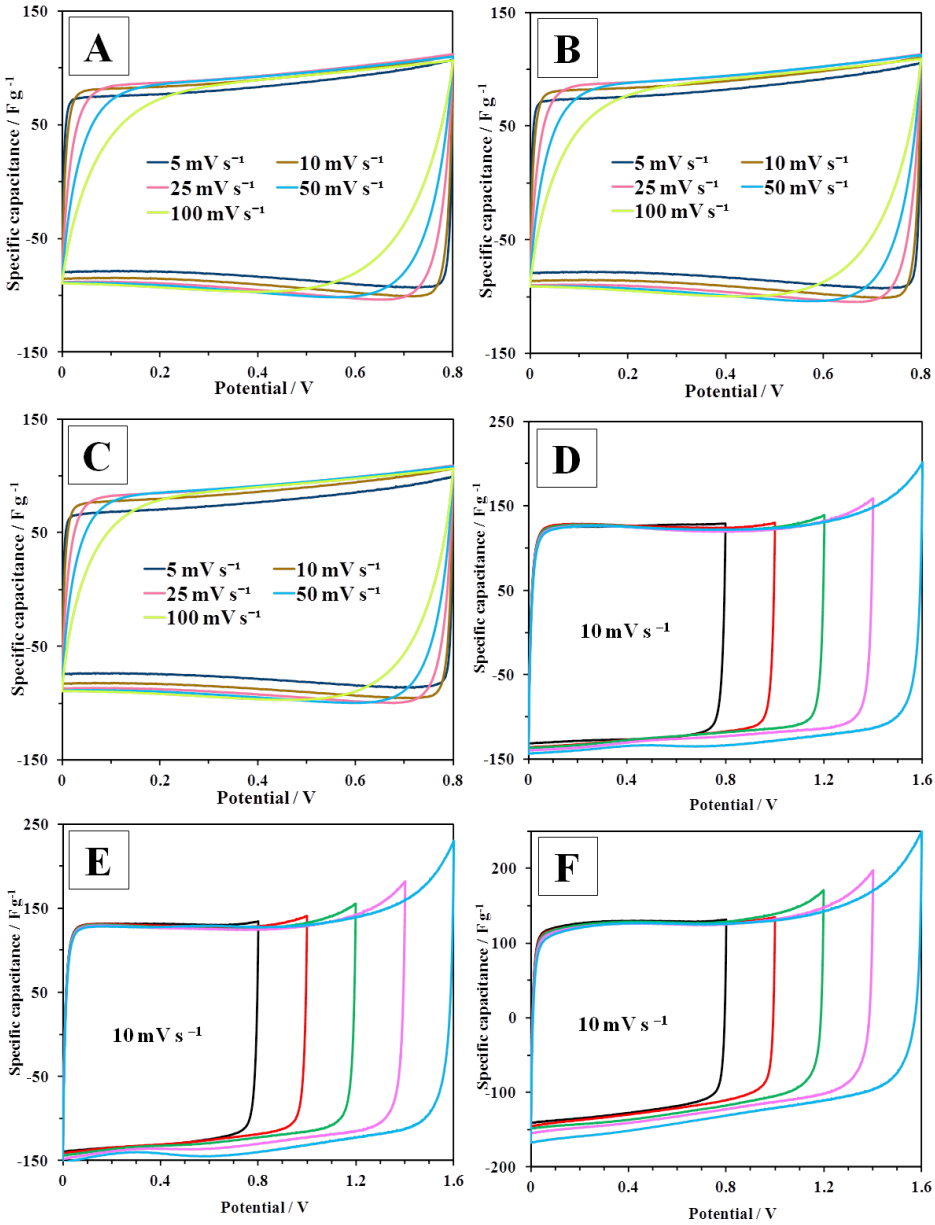

Figure 9. Cyclic voltammetry curves of electrochemical double layer capacitors (EDLCs) with (A) CS, (B) CS/SA PEC membrane and (C) Whatman GF/A glass fiber separator at different scan rates. Voltammograms of EDLCs with (D) CS, (E) CS/SA PEC membrane and (F) Whatman GF/A separator at different potential range (10 mV s^{-1}). Abbreviations: CS, chitosan; CS/SA PEC, chitosan/sodium alginate polyelectrolyte complex, GF/A, glass fibre.

higher values of specific capacitance than the reference test cell, and the trend is clearly visible for all applied potential ranges. These phenomena can be related to dimensional stability differences of the tested membranes discussed in section 3.4. The dimensional

DOI: 10.15259/PCACD.25.014

stability of the CS/SA PEC quasi-solid electrolyte caused by intermolecular interactions between CS and SA has a positive effect on the capacitance of the EDLC cell, despite the decreased membrane ionic conductivity after modification process (Table 1). The balance between electrolyte uptake and reduction of swelling means that the CS/SA PEC membrane ensures excellent penetration of the electrolyte into the pores of the electrode material while maintaining constant membrane dimensions. Moreover, analysis of CV curves recoded in expanded potential range (Figs. 9D–F) revealed that chitosan membrane modified with SA can be successfully applied at higher voltages because it maintains its excellent properties working without any trace of redox reactions, comparable even with commercially used Whatman GF/A separator.

3.6.3. GCD

The cyclical repeatability of the CS, CS/SA PEC and Whatman GF/A test cells was examined by a GCD method. Fig. 10 displays the GCD profiles in all used potential ranges. Detailed analysis of potential/time dependency curves showed that all registered GCD profiles exhibited a triangular shape for both the 1st and 1000th cycle. This is a typical

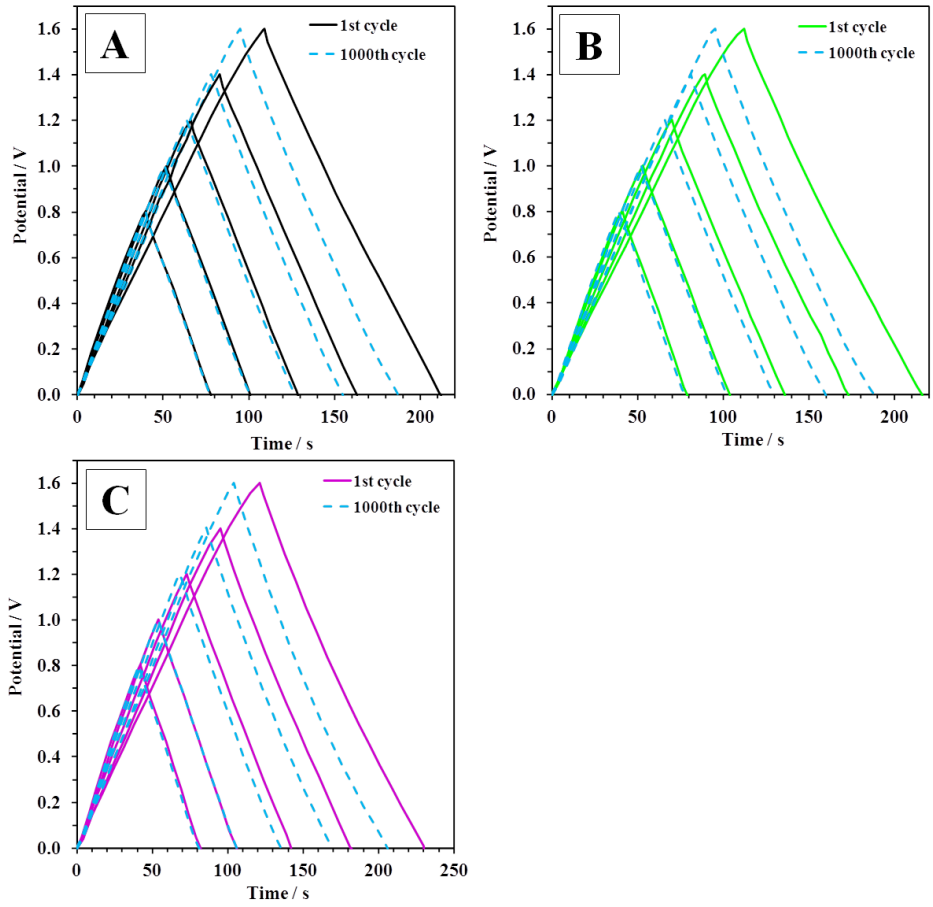

Figure 10. Galvanostatic charge/discharge curves at the 1st and 1000th cycle for electrochemical double layer capacitor (EDLC) cells with (A) CS, (B) CS/SA PEC membrane and (C) Whatman GF/A separator. Abbreviations: CS, chitosan; CS/SA PEC, chitosan/sodium alginate polyelectrolyte complex, GF/A, glass fibre.

characteristic for EDLCs; it indicates the non-Faradaic nature of the capacitive properties and good cyclic repeatability [39].

Of note, the 1000th cycle GCD profiles recorded for broader potential range (1.2 V inclusive) exhibited a slight shift of the curve relative to the initial ones. This phenomenon can be related to the well-known electro-decomposition of water particles (over 1.23 V) and is more visible for the CS/SA PEC EDLC test cell. It can affect the repeatability of the EDLCs, and thus future investigations should involve a long term GCD tests (over 10,000 cycles).

The specific capacitance values were obtained from the corresponding GCD curves according to:

$$C_{sp} = I/(\mathrm{d}U/\mathrm{d}t)m^{-1}, \quad (5)$$

where I is the discharge current, $\mathrm{d}U/\mathrm{d}t$ is the slope of the discharge curve and m is the mass of the electrode. Table 3 gives specific capacitance values obtained after the 1000th GCD cycle with a constant current of 5 mA, for all tested potential ranges and EDLC cells

Table 3 Specific capacitance (C_{sp}) of electrochemical double layer capacitor (EDLC) EDLC cells, calculated from a galvanostatic charge/discharge test after 1000th cycle.

EDLC	C_{sp} [F g^{-1}]				
	0 – 0.8 V	**0 – 1.0 V**	**0 – 1.2 V**	**0 – 1.4 V**	**0 – 1.6 V**
CS	100	104	109	114	122
CS/SA PEC	102	107	114	120	124
Whatman GF/A	99	104	111	119	125

Abbreviations: CS, chitosan; CS/SA PEC, chitosan/sodium alginate polyelectrolyte complex, GF/A, glass fibre.

The CS/SA PEC cell exhibited the highest specific capacitance values, in all applied potential ranges (from 102 F g^{-1} for 0–0.8 V to 124 F g^{-1} for 0–1.6 V). These results correspond with the values obtained by cyclic voltammetry and the trend shows a superior electrochemical performance of EDLC with the CS/SA PEC membrane over non-modified CS (C_{sp} values from 100 F g^{-1} for 0–0.8 V to 122 F g^{-1} for 0-1.6 V). Moreover, the specific capacitance values for the CS/SA PEC capacitor were comparable even with the Whatman GF/A cell (C_{sp} values from 99 F g^{-1} for 0–0.8 V to 125 F g^{-1} for 0-1.6 V). These results suggest that the CS/SA PEC quasi-solid electrolyte can be an alternative modification for CS-based materials of electrochemical purpose due to its excellent performance even in higher work potential (over 1.2 V) and good repeatability of charge/discharge cycles.

4. Conclusions

Following physicochemical characterization (using XRD, SEM and ATR-FTIR) the modification of the CS/SA PEC membrane was confirmed and then used in an EDLC cell to study it applicability as quasi-solid electrolyte. The results showed that the CS/SA PEC membrane saturated with aqueous 2 M Li_2SO_4 exhibits good dimensional stability and lower than reference chitosan sample ionic conductivity. The tested EDLC cell with a CS/SA PEC membrane exhibits good electrochemical performance and superior specific

capacitance compared to raw CS membrane and Whatman GF/A glass fiber separator reference cells. Thus, the CS/SA PEC quasi-solid electrolyte can be considered as an alternative modification for CS-based materials of electrochemical purpose.

5. Acknowledgements

This work was performed with the financial support of National Science Center, Poland (Grant No 2015/17B/ST8/00365) and Poznan University of Technology, Poland (Grant No. 0911/SBAD/0395/2020).

6. References

[1] Jacob J, Haponiuk J T, Thomas S, Gopi S; (2018) Biopolymer based nanomaterials in drug delivery systems: A review. Mater Today Chem 9, 43–55. **DOI:** 10.1016/j.mtchem.2018.05.002

[2] Yadav P, Yadav H, Shah V G, Shah G, Dhaka G; (2015) Biomedical Biopolymers, their Origin and Evolution in Biomedical Sciences: A Systematic Review. JCDR 9(9), 21–25. **DOI:** 10.7860/JCDR/2015/13907.6565

[3] Mogosanu G D, Grumezescu A M; (2014) Natural and synthetic polymers for wounds and burns dressing. Int J Pharm 463, 127–136. **DOI:** 10.1016/j.ijpharm.2013.12.015

[4] Caetano G F, Frade M A C, Thiago Andrade T A M, Leite M N, Bueno C Z, Moraes A M, Ribeiro-Paes J T; (2014) Chitosan-alginate membranes accelerate wound healing. J Biomed Mater Res Part B 103B, 1013–1022. **DOI:** 10.1002/jbm.b.33277

[5] Raman S P, Keil C, Dieringer P, Hübner C, Bueno A, Gurikov P, Nissen J, Holtkamp M, Karst U, Haase H, Smirnova I; (2019) Alginate aerogels carrying calcium, zinc and silver cations for woundcare: Fabrication and metal detection. J Supecrit Fluid 153, 104545. **DOI:** 10.1016/j.supflu.2019.104545

[6] Vernaez O, Neubert K J, Kopitzky R, Kabasci S; (2019) Compatibility of Chitosan in Polymer Blends by Chemical Modification of Bio-based Polyesters. Polymers 11, 1939. **DOI:** 10.3390/polym11121939

[7] Córdova B M, Jacinto C R, Alarcón H, Mejía I M, López R C, Silva D O, Cavalheiro E T G, Venâncio T, Dávalos J Z, Valderrama A C; (2018) Chemical modification of sodium alginate with thiosemicarbazide for the removal of Pb(II) and Cd(II) from aqueous solutions. Int J Biol Macromol 120, 2259–2270. **DOI:** 10.1016/j.ijbiomac.2018.08.095

[8] Nowacki K, Galiński M, Stępniak I; (2019) Synthesis and characterization of modified chitosan membranes for applications in electrochemical capacitor. Electrochim Acta 320, 134632. **DOI:** 10.1016/j.electacta.2019.134632

[9] Zhang R, Wang L, Zhao J, Guo S; (2019) Effects of Sodium Alginate on the Composition, Morphology, and Electrochemical Properties of Electrospun Carbon Nanofibers as Electrodes for Supercapacitors. ACS Sustainable Chem Eng 7, 632–640. **DOI:** 10.1021/acssuschemeng.8b04191

[10] Eldin M S M, Hashem A E, Tamer T M, Omer A M, Yossuf M E, Sabet M M; (2017) Development of Cross linked Chitosan/Alginate Polyelectrolyte Proton Exchanger Membranes for Fuel Cell Applications. Int J Electrochem Sci 12, 3840–3858. **DOI:** 10.20964/2017.05.45

[11] Liu C, Guo X, Cui H, Yuan R; (2009) An amperometric biosensor fabricated from electro-co-deposition of sodium alginate and horseradish peroxidase. J Mol Catal B-Enzym 60, 151–156. **DOI:** 10.1016/j.molcatb.2009.04.015

[12] Pillai C K S, Paul W, Sharma C P; (2009) Chitin and chitosan polymers: Chemistry, solubility and fiber formation. Prog Polym Sci 34, 641–678. **DOI:** 10.1016/j.progpolymsci.2009.04.001

[13] Bhattarai N, Gunn J, Zhang M; (2010) Chitosan-based hydrogels for controlled, localized drug delivery. Adv Drug Deliv Rev 62, 83–99. **DOI:** 10.1016/j.addr.2009.07.019

[14] Kumar M S, Bhat D K; (2009) $LiClO_4$-Doped Plasticized Chitosan as Biodegradable Polymer Gel Electrolyte for Supercapacitors. J Appl Polym Sci 114, 2445–2454. **DOI:** 10.1002/app.30716

[15] Kotatha D, Torii Y, Shinomiya K, Ogino M, Uchida S, Ishikawa M, Furuike T, Tamura H; (2019) Preparation of thin-film electrolyte from chitosan-containing ionic liquid for application to electric double-layer capacitors. Int J Biol Macromol 124, 1274–1280. **DOI:** 10.1016/j.ijbiomac.2018.12.006

[16] Berger J, Reist M, J.M. Mayer J M, Felt O, Peppas N A, Gurny R; (2004) Structure and interactions in covalently and ionically crosslinked chitosan hydrogels for biomedical applications. Eur J Pharm Biopharm 57, 19–34. **DOI:** 10.1016/S0939-6411(03)00161-9

[17] Yang C, Dan N, You W, Huang Y, Chen Y, Yu G, Dan W, Wen H; (2019) Modification of collagen-chitosan membrane by oxidation sodium alginate and *in vivo/ in vitro* evaluation for wound dressing application. Int J Polym Anal Ch, 24:7, 619–629, **DOI:** 10.1080/1023666X.2019.1648637

[18] Sanaa A, Boulila A, Boussaid M, Fadhel N B; (2013) Alginic acid and derivatives, new polymers from the endangered *Pancratium maritimum* L.. Ind Crops Prod 44, 290–293. **DOI:** 10.1016/j.indcrop.2012.11.014

[19] Vreeland V, Laetsch W M; (1989) Identification of associating carbohydrate sequences with labelled oligosaccharides. Planta 177, 423–434. **DOI:** 10.1007/BF00392610

[20] Xie, C-X, Tian T-C, Yu S-T, Li L; (2019) pH-sensitive hydrogel based on carboxymethyl chitosan/sodium alginate and its application for drug delivery. J Appl Polym Sci 136:1, 46911. **DOI:** 10.1002/APP.46911

[21] Prabha G, Raj V; (2017) Sodium alginate–polyvinyl alcohol–bovin serum albumin coated Fe_3O_4 nanoparticles as anticancer drug delivery vehicle: Doxorubicin loading and in vitro release study and cytotoxicity to HepG2 and L02 cells. Mater Sci Eng C 79, 410–422. **DOI:** 10.1016/j.msec.2017.04.075

[22] Yeom C K, Lee K-H; (1997) Vapor permeation of ethanol-water mixtures using sodium alginate membranes with crosslinking gradient structure. J Membrane Sci 135, 225–235. **DOI:** 10.1002/(SICI)1097-4628(19980822)69:8<1607::AID-APP15>3.0.CO;2-R

[23] Zhang L, Guo J, Zhou J, Yang G, Du Y; (2000) Blend Membranes from Carboxymethylated Chitosan/Alginate In Aqueous Solution. J Appl Polym Sci 77, 610–616. **DOI:** 10.1002/(SICI)1097-4628(20000718)77:3<610::AID-APP16>3.0.CO;2-B

[24] Yang H, Ji X, Tan Y, Liu Y, Ran F; (2019) Modified supramolecular carboxylated chitosan as hydrogel electrolyte for quasi-solid-state supercapacitors. J Power Sources 441, 227174. **DOI:** 10.1016/j.jpowsour.2019.227174

[25] Lijuan K, Ruiyi L, Yongqiang Y, Zaijun L; (2016) Multi-faceted design of a silicon anode for high performance lithium ion batteries using silicon nanoparticles encapsulated by a multiple grapheme aerogel electrode material and a tryptophan-functionalized graphene quantum dot–sodium alginate binder. RSC Adv 6, 76344. **DOI:** 10.1039/c6ra15257k

[26] Shaari N, Kamarudin S K; (2015) Chitosan and alginate types of bio-membrane in fuel cell application: An overview. J Power Sources 289, 71–80. Doi: 10.1016/j.jpowsour.2015.04.027

[27] Jiang C, Wang Z, Zhang X, Zhu X, Nie J, Ma J; (2014) Crosslinked polyelectrolyte complex fiber membrane based on chitosan–sodium alginate by freeze-drying. RSC Adv 4, 14551. **DOI:** 10.1039/c4ra04208e

[28] Kim S-G, Lee K-S, Lee K-H; (2007) Pervaporation Separation of Sodium Alginate/ Chitosan Polyelectrolyte Complex Composite Membranes for the Separation of Water/Alcohol Mixtures: Characterization of the Permeation Behavior with Molecular Modeling Techniques. J Appl Polym Sci 103, 2634–2641. **DOI:** 10.1002/ app.25386

[29] Lee K Y, Park W H, Ha W S; (1997) Polyelectrolyte Complexes of Sodium Alginate with Chitosan or Its Derivatives for Microcapsules. J Appl Polym Sci 63:4, 425–432. **DOI:** 10.1002/(SICI)1097-4628(19970124)63:4<425::AID-APP3>3.0.CO;2-T

[30] Meng X, Tian F, Yang J, He C-N, Xing N, Li F; (2010) Chitosan and alginate polyelectrolyte complex membranes and their properties for wound dressing application. J Mater Sci: Mater Med 21, 1751–1759. **DOI:** 10.1007/s10856-010-3996-6

[31] Gierszewska M, Ostrowska-Czubenko J, Chrzanowska E; (2018) pH-responsive chitosan/alginate polyelectrolyte complex membranes reinforced by tripolyphosphate. Eur Polym J 101, 282–290. **DOI:** 10.1016/j.eurpolymj.2018.02.031

[32] Bierhalz A C K, Westin C B, Moraes A M; (2016) Comparison of the properties of membranes produced with alginate and chitosan from mushroom and from shrimp. Int J Biol Macromol 91, 496–504. **DOI:** 10.1016/j.ijbiomac.2016.05.095

[33] Smitha B, Sridhar S, Khan A A; (2005) Chitosan–sodium alginate polyion complexes as fuel cell membranes. Eur Polym J 41, 1859–1866. **DOI:** 10.1016/j. eurpolymj.2005.02.018

[34] Han J, Wang H, Yue Y, Mei C, Chen J, Huang C, Wu Q, Xu X; (2019) A self-healable and highly flexible supercapacitor integrated by dynamically cross-linked electro-conductive hydrogels based on nanocellulose-templated carbon nanotubes embedded in a viscoelastic polymer network. Carbon 149, 1–18. **DOI:** 10.1016/j. carbon.2019.04.029

[35] Sudhakar Y N, Selvakumar M; (2012) Lithium perchlorate doped plasticized chitosan and starch blend as biodegradable polymer electrolyte for supercapacitors. Electrochim Acta 78, 398–405. **DOI:** 10.1016/j.electacta.2012.06.032

[36] Tõnurist K, Thomberg T, Jänes A, Kink I, Lust E; (2012) Specific performance of electrical double layer capacitors based on different separator materials in room temperature ionic liquid. Electrochem Commun 22, 77–80. **DOI:** 10.1016/j. elecom.2012.05.029

[37] Virya A, Lian K; (2017) Li_2SO_4-polyacrylamide polymer electrolytes for 2.0 V solid symmetric supercapacitors. Electrochem Commun 81, 52–55. **DOI:** 10.1016/j. elecom.2017.06.003

[38] Abbas Q, Beguin F; (2016) High voltage AC/AC electrochemical capacitor operating at low temperature in salt aqueous electrolyte. J Power Sources 318, 235–241. **DOI:** 10.1016/j.jpowsour.2016.03.088

[39] Gao Q, Demarconnay L, Raymundo-Pinero E, Beguin F; (2012) Exploring the large voltage range of carbon/carbon supercapacitors in aqueous lithium sulfate electrolyte. Energy Environ Sci 5, 9611–9617. **DOI:** 10.1039/c2ee22284a